

Fermionic full counting statistics with smooth boundaries: from discrete particles to bosonization

Dmitri A. Ivanov^{1,2} and Ivan P. Levkivskyi^{1,3}

¹*Institute for Theoretical Physics, ETH Zürich, 8093 Zürich, Switzerland*

²*Institute for Theoretical Physics, University of Zürich, 8057 Zürich, Switzerland*

³*Bogolyubov Institute for Theoretical Physics, 14-b Metrolohichna Street, Kyiv 03680, Ukraine*

(Dated: July 24, 2015)

We revisit the problem of full counting statistics of particles on a segment of a one-dimensional gas of free fermions. Using a combination of analytical and numerical methods, we study the crossover between the counting of discrete particles and of the continuous particle density as a function of smoothing in the counting procedure. In the discrete-particle limit, the result is given by the Fisher–Hartwig expansion for Toeplitz determinants, while in the continuous limit we recover the bosonization results. This example of full counting statistics with smoothing is also related to orthogonality catastrophe, Fermi-edge singularity and non-equilibrium bosonization.

Introduction.— Full counting statistics (FCS), in theoretical-condensed-matter context, refers to a class of problems involving the probability distribution of a quantum observable (usually the number of electrons found in a certain region of space or transported through the system over a certain time) with a particular focus on quantum behavior. Examples of FCS problems are the anti-bunching of electrons in a one-dimensional conductor due to their fermionic statistics [1, 2] and a single-electron emitter, first proposed theoretically [3] and recently realized experimentally [4].

The simplest FCS problems assume non-interacting fermions (electrons), so that the resulting counting statistics can be expressed in terms of a determinant taking into account antisymmetrization of the relevant multi-particle processes [1]. An alternative approach is based on the bosonization technique (using the equivalence between bosons and fermions in one dimension) [6]. Bosonization methods for FCS can be extended to include interactions, but they usually do not fully take into account the discreteness of particles [2, 7–9].

It is therefore important to understand limitations of the bosonization approach to FCS and its connection to the exact calculation with discrete fermions. In this Letter, we address this problem by studying FCS in a one-dimensional free-fermion model, where an uncertainty (smoothing) in the counting procedure is introduced, so that the particle number is no longer quantized. In this model, we can study in full detail a crossover between the discrete-particle and bosonization results as the uncertainty increases. While the details of this crossover depend on the profile of the introduced uncertainty, the qualitative description of the crossover is found to be universal: FCS respects the discreteness of particles if the uncertainty region is much narrower than the (average) inter-particle distance, but crosses over to the bosonization result when the uncertainty region is much wider than the inter-particle distance.

Mathematically, this problem amounts to studying

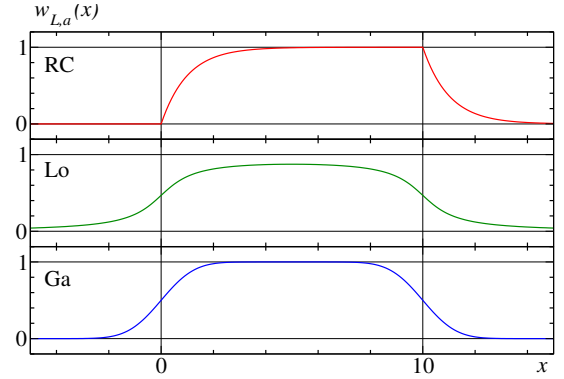


FIG. 1: The weight functions $w_{L,a}(x)$ for $L = 10$ and $a = 1$ for the three models of smoothing.

an evolution of the asymptotic behavior of a Toeplitz (or, more precisely, Wiener–Hopf) determinant with a Fisher–Hartwig singularity [10, 11] as the singularity is smoothed in a certain way. In the case of a sharp singularity, the corresponding determinant is given by a double asymptotic series of a Fisher–Hartwig type fully respecting the particle discreteness [18, 20]. As the singularity is smoothed, the secondary branches of this expansion get suppressed, and the remaining leading branch reproduces the bosonization result.

Model.— We consider the one-dimensional model of spinless free fermions on a line (both coordinate and momentum are continuous) at zero temperature. The system is in its ground state, which is the Slater determinant of plane waves characterized by the Fermi wave vector k_F : the states with the wave vectors smaller than k_F (in absolute value) are occupied, and the states with the wave vectors larger than k_F are empty. We introduce the FCS generating function as [1, 5]

$$\chi_{L,a}(\kappa) = \langle \exp(2\pi i \kappa Q_{L,a}) \rangle, \quad (1)$$

where the average is taken over the ground state. The particle-counting operator $Q_{L,a}$ is defined as

$$Q_{L,a} = \int_{-\infty}^{\infty} \Psi^\dagger(x) \Psi(x) w_{L,a}(x) dx, \quad (2)$$

where $\Psi^\dagger(x)$ and $\Psi(x)$ are the fermionic creation and annihilation operators and $w_{L,a}(x)$ is the weight function for the particle counting. The weight function depends on the two parameters: the length of the interval L and the smoothing length scale a , Fig. 1. We always assume $L \gg a$.

In the original formulation of the FCS problem, the smoothing is absent ($a = 0$), and the weight function is the characteristic function of a line segment,

$$w_{L,0}(x) = \theta(x)\theta(L-x) = \begin{cases} 0 & x < 0 \text{ or } x > L, \\ 1 & 0 < x < L. \end{cases} \quad (3)$$

In this case, $Q_{L,a}$ takes integer values, and the generating function (1) is periodic in the counting variable, $\chi_{L,0}(\kappa+1) = \chi_{L,0}(\kappa)$. It can be expressed as a Toeplitz determinant (see Appendix), which has been subject to extensive studies [12–17]. The periodicity of $\chi_{L,0}(\kappa)$ is reflected in a Fisher–Hartwig-type asymptotic series (conjectured and numerically verified to a very high order) [18–21]:

$$\chi_{L,0}(\kappa) = \sum_{j=-\infty}^{\infty} \tilde{\chi}_{L,0}(\kappa+j), \quad (4a)$$

$$\tilde{\chi}_{L,0}(\kappa) = \exp \left[2\pi i \kappa N_L - 2\kappa^2 \ln(2\pi N_L) + \tilde{C}(\kappa) + \sum_{n=1}^{\infty} f_n(\kappa) (iN_L)^{-n} \right]. \quad (4b)$$

The coefficients in this double expansion can be explicitly calculated: $\tilde{C}(\kappa)$ is expressed in terms of Barnes G functions as $\tilde{C}(\kappa) = 2\ln|G(1+\kappa)G(1-\kappa)|$, and $f_n(\kappa)$ are polynomials in κ , which can be computed iteratively, order by order [20] (the same coefficients are denoted $P_{nn}(\kappa)$ in [21]). $\chi_{L,0}(\kappa)$ depends only on one parameter: the average particle number on the segment,

$$N_L = k_F L / \pi. \quad (5)$$

On the other hand, a bosonization approach proposed for the generating function $\chi_{L,a}(\kappa)$ [2] leads to

$$\chi_{L,a}^{\text{bos}}(\kappa) = \exp \left(2\pi i \kappa N_L - 2\kappa^2 [\ln(N_L/N_a) + \text{const}] \right), \quad (6)$$

where we have defined the average number of particles in the smoothing region

$$N_a = k_F a / \pi, \quad (7)$$

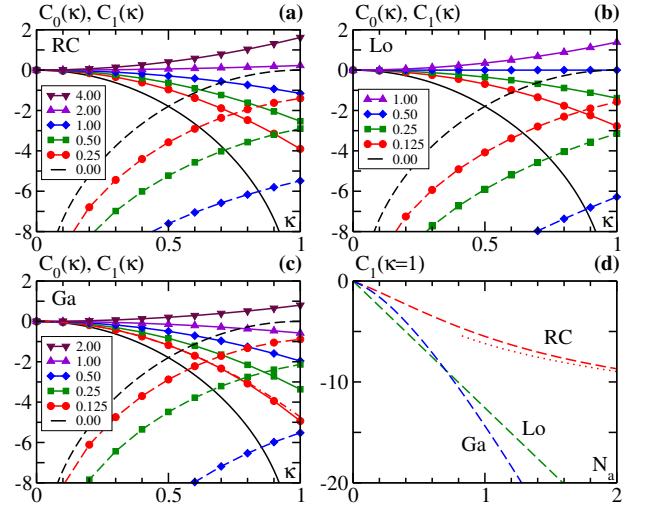


FIG. 2: **(a)–(c)**: Coefficients $C_0(\kappa, a)$ and $C_1(\kappa, a)$ as a function of κ for several values of N_a , as computed from numerical fits. $C_0(\kappa, a)$ are shown by solid lines, $C_1(\kappa, a)$ by dashed lines. Different symbols correspond to different values of N_a as shown in the legends. In panel (c), the dash-dotted line is the bosonization result (12) at $N_a = 0.125$. **(d)**: Coefficient $C_1(\kappa=1, a)$ as a function of N_a for the three models. The plot for Lo model is the exact analytical result (20). The dotted line is the leading asymptotics (19) for RC model.

and the constant at the logarithm depends on the details of the smoothing. The bosonization expression (6) corresponds to the leading terms in the leading branch ($j = 0$) of the double expansion (4). We expect (and confirm it the present work) that this result applies provided the smoothing a is sufficiently large. It is not periodic in κ , which is consistent with a continuous spectrum of the operator $Q_{L,a}$ at a finite a .

The goal of the present study is to examine in detail the crossover from the discrete particle counting given by the expansion (4) to the bosonization result (6) as a function of the smoothing parameter a . Some of the results are derived analytically, while a more detailed picture of the crossover is obtained numerically. Smoothing is introduced as a convolution

$$w_{L,a}(x) = \int_{-\infty}^{\infty} \frac{dx'}{a} \theta(x)\theta(L-x) g(x'/a), \quad (8)$$

where $g(\tilde{x})$ is a smoothing function for the scaled coordinate $\tilde{x} = x/a$. We always assume the normalization $\int d\tilde{x} g(\tilde{x}) = 1$. To be specific, we consider three models of smoothing corresponding to the three choices of the smoothing function: RC (this type of smoothing may be relevant for particle-counting in time, where the counter has a RC-type response function), Lorentzian (Lo) and Gaussian (Ga):

$$g(\tilde{x}) = \begin{cases} \theta(\tilde{x}) \exp(-\tilde{x}) & \text{RC,} \\ [\pi(\tilde{x}^2 + 1)]^{-1} & \text{Lo,} \\ \exp(-\tilde{x}^2/2)/\sqrt{2\pi} & \text{Ga} \end{cases} \quad (9)$$

(see Fig. 1). In any of these models, the FCS generating function $\chi_{L,a}(\kappa)$ depends on L and a via the two dimensionless parameters N_L and N_a .

Results.— We conjecture (and support this conjecture by analytical and numerical results) that, at a finite a , the FCS generating function admits the same structure of the expansion (4) as at $a = 0$, except that the expansion coefficients are not periodic in the branch index j and depend on the smoothing parameter a . If we limit the range of κ to the interval $[0, 1]$, we can write the leading terms of the expansion as

$$\begin{aligned} \chi_{L,a}(\kappa) \approx & \exp \left[2\pi i \kappa N_L - 2\kappa^2 \ln N_L + C_0(\kappa, a) \right] \\ & + \exp \left[2\pi i (\kappa - 1) N_L - 2(\kappa - 1)^2 \ln N_L + C_1(\kappa, a) \right]. \end{aligned} \quad (10)$$

At $a = 0$, in agreement with the full expansion (4), the coefficients $C_0(\kappa, a)$ and $C_1(\kappa, a)$ are given by

$$\begin{aligned} C_0(\kappa, 0) &= C_1(1 - \kappa, 0) \\ &= 2 \ln |G(1 + \kappa)G(1 - \kappa)| - 2\kappa^2 \ln(2\pi). \end{aligned} \quad (11)$$

We expect that, as a increases, $C_0(\kappa, 0)$ also increases to reproduce the bosonization result (6), while $C_1(\kappa, 0)$ decreases to suppress the second term in the expansion (10).

This behavior is indeed confirmed by numerical studies. We report the details of our numerics in the Appendix, and here we only plot in Fig. 2a-c the results of the numerical fits for the coefficients $C_0(\kappa, a)$ and $C_1(\kappa, a)$ for the three models of the smoothing. Figure 2d shows more detailed results for the coefficient $C_1(1, a)$ representing the suppression of the secondary Fisher–Hartwig branch at $\kappa = 1$. This coefficient was, in fact, computed as a doubled contribution from a single “phase slip” (at the beginning or at the end of the interval) in the weight function $w_{L,a}(x)$ (note that at $\kappa = 1$ the values $w_{L,a}(x) = 0$ and $w_{L,a}(x) = 1$ are equivalent, see Appendix). An agreement between the results computed with this method (at $\kappa = 1$) and the fitting procedure for the full function $\chi_{L,a}(\kappa)$ serves as an independent check of our numerical scheme.

As expected, while the actual values of the coefficients $C_0(\kappa, a)$ and $C_1(\kappa, a)$ depend on the chosen smoothing model, qualitatively the crossover between the discrete particle counting and a continuous bosonization description occurs at $N_a \sim 1$ in all the three models.

Furthermore, some of the numerical results presented above can be verified by analytical means. First, the constant in the bosonization formula (6) can be computed from the corresponding Toeplitz determinant using the strong Szegő theorem [22, 23]. This results in the asymptotic behavior for $C_0(\kappa, a)$:

$$C_0(\kappa, a \rightarrow \infty) = 2\kappa^2 (\ln N_a - \Upsilon), \quad (12)$$

where

$$\Upsilon = \gamma + \lim_{\varepsilon \rightarrow 0} \left[\int_{\varepsilon}^{\infty} \frac{dk}{k} g_k g_{-k} + \ln \varepsilon \right], \quad (13)$$

in the case of a general smoothing model (8). Here $\gamma = 0.5772\dots$ is the Euler–Mascheroni constant and g_k are the Fourier components of the smoothing function,

$$g_k = \int_{-\infty}^{\infty} d\tilde{x} e^{-ik\tilde{x}} g(\tilde{x}). \quad (14)$$

For the three models considered in our paper, a calculation gives

$$\Upsilon_{\text{RC}} = \gamma, \quad \Upsilon_{\text{Lo}} = -\ln 2, \quad \Upsilon_{\text{Ga}} = \gamma/2. \quad (15)$$

These analytical results perfectly agree with our numerical fits: for the RC and Lorentzian smoothing, the computed values of $C_0(\kappa, a)$ for $N_a \geq 0.25$ and $N_a \geq 0.125$, respectively, are indistinguishable in the plots of Fig. 2a,b from the bosonization asymptotics (12), (15). For the Gaussian smoothing, the difference between $C_0(\kappa, a)$ and the bosonization asymptotics is visible for $N_a = 0.125$, but not for $N_a \geq 0.25$ (Fig. 2c).

Second, the asymptotic behavior of $C_1(1, a)$ as $a \rightarrow \infty$ can also be calculated analytically using an asymptotic formula for the Toeplitz determinant with a non-zero winding number [24]. A calculation results in

$$\begin{aligned} \frac{1}{2} C_1(1, a \rightarrow \infty) &\approx \Xi - \Upsilon \\ &+ \text{Re} \ln \int_{-\infty}^{\infty} \frac{dz}{2\pi} \exp \left[2\pi i N_a z - \int_{-\infty}^{\infty} dk g_k \frac{1 - e^{ikz}}{|k|} \right], \end{aligned} \quad (16)$$

where Υ is given by (13) and Ξ is defined as

$$\Xi = 2\gamma + \lim_{\varepsilon \rightarrow 0} \left[\int_{\varepsilon}^{\infty} \frac{dk}{k} (g_k + g_{-k}) + 2 \ln \varepsilon \right]. \quad (17)$$

An explicit calculation gives

$$\Xi_{\text{RC}} = 2\gamma, \quad \Xi_{\text{Lo}} = 0, \quad \Xi_{\text{Ga}} = \gamma + \ln 2. \quad (18)$$

Remarkably, the asymptotics (16), while not exactly coinciding with $C_1(1, a)$, gives a very good approximation in the whole range of the values of a (in the plot in Fig. 2d it would be indistinguishable from the exact values, see details in Appendix).

The analytic approximation (16) also allows us to extract the leading asymptotic behavior. For the RC model, we find

$$C_1(1, a \rightarrow \infty)_{\text{RC}} \approx 2\gamma - 4 \ln(2\pi N_a), \quad (19)$$

i.e., the secondary branch of $\chi(1, a)$ decays as N_a^{-4} . For the Lorentzian smoothing, the Toeplitz determinant for

a single “phase slip” $w_a(x) = \frac{1}{2\pi i} \ln\left(\frac{x+ia}{x-ia}\right)$ may be computed exactly by using the analyticity of the function $\exp[2\pi w_a(x)]$ in one of the half-planes. An argument in the spirit of [3, 25] then leads to the exact result:

$$C_1(1, a)_{\text{Lo}} = -4\pi N_a. \quad (20)$$

Finally, for the Gaussian smoothing, the asymptotic behavior is

$$C_1(1, a \rightarrow \infty)_{\text{Ga}} \sim -4\pi N_a \sqrt{\ln(2\pi N_a^2)}. \quad (21)$$

However, this expression by itself [unlike the integral formula (16)] does not provide a good approximation for $C_1(1, a)$, since the next-order corrections are not $O(1)$.

Remarkably, even though the coefficient at the secondary branch is reduced with increasing N_a , the dependence on N_L does not change. In particular, for $\kappa > 1/2$, the bosonization (first) term in (10) always decreases with N_L faster than the non-bosonization (second) one. This implies that the non-bosonization corrections arising from the discreteness of particles should be visible, in this range of κ , at sufficiently large L (see Appendix). The corresponding values of L depend on the particular choice of smoothing and can be deduced from comparing the two terms in (10) using the asymptotics at large N_a derived above. A practical observation of this effect may be limited at large N_a if both terms in (10) become too small.

Discussion.— In this Letter, we have discussed the crossover from discrete to continuous FCS in the model of free one-dimensional fermions, as a function of smoothing. This model may serve as an illustration of a relation between discrete and continuous descriptions in a wide spectrum of similar problems, including FCS with temporal measurements, Fermi-edge singularity, orthogonality catastrophe, and non-equilibrium bosonization.

By FCS with temporal measurements we understand a FCS setup where the counting is performed over a certain time interval, e.g., by opening and closing an electric contact or by applying a time-dependent voltage pulse [1, 2]. This formulation of FCS used in the original FCS papers differs from our approach where the measurement is extended in space instead of time. This difference implies the necessity of regularizing the contribution of the Fermi sea in temporal FCS: a large current of left-movers is compensated by a similarly large current of right-movers, so the average charge transfer is determined by the vicinity of the Fermi level, while the quantum noise depends on the ultraviolet cutoff defined by the Fermi energy ε_F (arising from the bottom of the Fermi sea). In our spatial formulation, there is no cutoff introduced by the bottom of the Fermi sea, and both the total number of particles and its fluctuations depend on the same scale k_F . As a consequence of this difference in ultraviolet cutoffs, our results cannot be literally translated to the case of temporal FCS. However, we expect that the main qualitative conclusion will hold also in the temporal case: the

generating function $\chi(\kappa)$ loses periodicity in κ when the smoothing time scale exceeds the typical time between particles (i.e., ε_F^{-1}).

Determinants similar to the generating function $\chi(\kappa)$ also appear in problems related to the orthogonality catastrophe and to the Fermi-edge singularity (FES). In those cases, the counterparts of the secondary branches of $\chi(\kappa)$ are secondary singularities (cusps or peaks) in the frequency-dependent response function (the closed-loop contribution in the FES context). Such secondary cusps and peaks were studied, e.g., in the recent work [26] (and, in the case of a bound-state contribution, earlier in [27]). According to our predictions, such cusps and peaks should be most visible in case of instant switching of the scattering potential, but get suppressed if the switching time of the scattering potential exceeds ε_F^{-1} .

We should also remark that most studies of FES involve an artificial regularization of the Fermi-sea contribution at energy scales smaller than ε_F , so that secondary singularities in the response function are neglected [28–30]. Such secondary singularities (separated from the main peak by ε_F) are probably not experimentally relevant in physical metals, where ε_F is a large energy scale, but may be of interest in other models with FES physics where ε_F is, for some reason, small (see, e.g., Ref. [31] for an example from spin-liquid theory).

Finally, we also mention recent works on non-equilibrium bosonization where determinants similar to ours appear (again, in the temporal form) [8]. Similarly to the FES problem discussed above, these works assume a regularization of the Fermi-sea contribution, which is equivalent to neglecting the secondary branches of the Fisher–Hartwig expansion related to the bottom of the Fermi sea.

Acknowledgment.— The authors are grateful to A. G. Abanov, E. Demler, M. V. Feigelman, L. Glazman, L. Levitov, A. Mirlin, and E. V. Sukhorukov for helpful discussions. The work of D.A.I. was supported by the Swiss National Foundation through the NCCR QSIT. I.P.L. was supported by Marie Curie Actions CO-FUND program.

APPENDIX

A. Toeplitz determinant for $\chi(\kappa)$.— The FCS generating function (1) can be written as a trace in the multi-particle space and then re-expressed as a determinant in the single-particle space [1, 2, 32]:

$$\chi_{L,a}(\kappa) = \det \left[(1 - n_F) + n_F e^{2\pi i \kappa w} \right], \quad (22)$$

where n_F is the Fermi occupation number and w is the operator of multiplication by $w_{L,a}(x)$. The operator n_F is diagonal in the momentum space, while w is diagonal in the coordinate space. In this paper, we consider the zero-

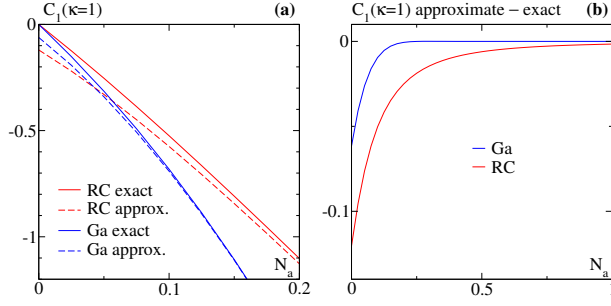


FIG. 3: **(a)** the values of $C_1(\kappa=1, a)$ for RC and Ga models (the same as in Fig. 2d) as calculated numerically, together with the analytic approximations given by (16). **(b)** the difference between the approximate and exact values of $C_1(\kappa=1, a)$ (upper curve: Ga model, lower curve: RC model).

temperature case, so n_F is a projector onto the occupied states (below k_F).

In the limit of no smoothing ($a = 0$), w is also a projector (in the coordinate space), and the determinant is symmetric with respect to exchanging coordinate and momentum:

$$\chi_{L,0}(\kappa) = \det [1 - (1 - e^{2\pi i \kappa}) n_F w]. \quad (23)$$

This operator is of Toeplitz (or Wiener-Hopf) form in both coordinate and momentum representations.

After introducing smoothing, the operator in (22) is no longer Toeplitz in the coordinate representation, but remains Toeplitz in the momentum representation (at zero temperature),

B. Toeplitz determinant for $C_1(\kappa=1, a)$.— At $\kappa = 1$, the term with $C_1(\kappa, a)$ in the decomposition (10) does not oscillate with L . It therefore arises from the end points of the segment of measurement ($x = 0$ and $x = L$). This allows us to calculate $C_1(\kappa=1, a)$ directly from a single-step contribution:

$$\frac{1}{2} C_1(\kappa=1, a) = \text{Re} \ln \det [(1 - n_F) + n_F e^{2\pi i \tilde{w}}], \quad (24)$$

where \tilde{w} is the operator of multiplication by the single-step counterpart of $w_{L,a}(x)$:

$$\tilde{w}_a(x) = \int_{-\infty}^{\infty} \frac{dx'}{a} \theta(x) g(x'/a). \quad (25)$$

Note that while $\tilde{w}_a(x)$ has different limits at $x \rightarrow \pm\infty$, the exponent $\exp(2\pi i \tilde{w})$ tends to 1 in both limits, and the determinant (24) is well defined.

C. Details of the numerical calculation.— For numerical calculations of $\chi_{L,a}(\kappa)$ and $C_1(\kappa=1, a)$, we approximate the integral operators (22) and (24) by finite-dimensional matrices by discretizing the momentum space (which is equivalent to considering the system on a circle). In the momentum space, these matrices are of Toeplitz form. The determinants of those matrices are

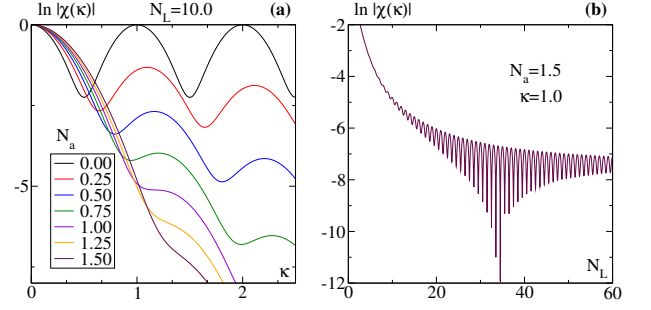


FIG. 4: **(a)** $\ln |\chi_{L,a}(\kappa)|$ as a function of κ in the RC model at $N_L = 10$ for selected values of N_a . Periodicity in κ is lost with increasing N_a . **(b)** $\ln |\chi_{L,a}(\kappa)|$ as a function of N_L in the RC model at $\kappa = 1$ and $N_a = 1.5$. For large N_L , the second term in (10) dominates.

calculated numerically for several matrix sizes and then extrapolated to the infinite matrix size in order to obtain $\chi_{L,a}(\kappa)$ and $C_1(\kappa=1, a)$, respectively.

For numerical calculations of the determinants, we use the LAPACK library [33], and Fourier transformations necessary for computing the matrix elements were done with the help of the GNU scientific library [34]. In our calculations, determinants of matrices of the linear size up to 600 were calculated, which allowed us to achieve good precision for the considered ranges of parameters.

The values of $\chi_{L,a}(\chi)$ were then fitted to the expansion (10), and the coefficients $C_0(\kappa, a)$ and $C_1(\kappa, a)$ were extracted (the fit also included terms up to L^{-2} in the exponents). As an additional check of this fitting procedure, we have verified that the values of $C_1(\kappa=1, a)$ obtained from these fits agree with those calculated independently using the one-step method described above.

D. Analytic approximation for $C_1(\kappa=1, a \rightarrow \infty)$.— The approximation (16), while derived under the assumption $N_a \gg 1$, is remarkably accurate even at small N_a . In the Lo model, where $C_1(\kappa=1, a)$ is given exactly by (20), the approximation (16) reproduces the same exact result for all N_a . In the RC and Ga models, the difference between (16) and $C_1(\kappa=1, a)$ tends to zero as $a \rightarrow \infty$, but remains finite at finite a . However, this difference is numerically small for these two models, even at $a = 0$. We plot this difference as a function of N_a in Fig. 3.

E. Numerical illustration of the crossover.— We illustrate the crossover described in the main body of the paper by two plots. In Fig. 4a, we show how the periodicity of $\chi_{L,a}(\kappa)$ in κ is gradually lost as N_a increases. Figure 4b illustrates how the second term in (10) dominates at large L (in RC model, for $\kappa = 1$, this happens at $L \gg k_F^2 a^3$).

[1] L. S. Levitov and G. B. Lesovik, Pisma v ZhETF **58**, 225 (1993) [JETP Lett. **58**, 230 (1993)],

- Charge distribution in quantum shot noise.*
- [2] L. S. Levitov, H.-W. Lee, and G. B. Lesovik, J. Math. Phys. **37**, 4845 (1996),
Electron Counting Statistics and Coherent States of Electric Current.
- [3] D. A. Ivanov, H. W. Lee, and L. S. Levitov, cond-mat/9501040, Phys. Rev. B **56**, 6839 (1997).
Coherent states of alternating current.
- [4] J. Dubois et al, Nature **502**, 659 (2013).
Minimal-excitation states for electron quantum optics using levitons.
- [5] V. E. Korepin, N. M. Bogoliubov, and A. G. Izergin, *Quantum Inverse Scattering Method and Correlation Functions* (Cambridge University Press, Cambridge, 1993) and references therein.
- [6] M. Stone, *Bosonization* (World Scientific, 1994);
A. O. Gogolin, A. A. Nersisyan, and A. M. Tsvelik, *Bosonization in strongly correlated systems*, (University Press, Cambridge 1998);
T. Giamarchi, *Quantum physics in one dimension*, (Clarendon Press Oxford, 2004).
- [7] I. P. Levkivskiy and E. V. Sukhorukov, Phys. Rev. Lett. **103**, 036801 (2009).
Noise-induced phase transition in the electronic Mach-Zehnder interferometer.
A. Helzel, L. V. Litvin, I. P. Levkivskiy, E. V. Sukhorukov, W. Wegscheider, and C. Strunk, Phys. Rev. B **91**, 245419 (2015).
Counting statistics and dephasing transition in an electronic Mach-Zehnder interferometer.
- [8] D. B. Gutman, Y. Gefen, and A. D. Mirlin, Europhys. Lett. **90**, 37003 (2010).
Bosonization out of equilibrium.
Phys. Rev. B **81**, 085436 (2010).
Bosonization of one-dimensional fermions out of equilibrium.
- [9] I. P. Levkivskiy and E. V. Sukhorukov, Phys. Rev. Lett. **109**, 246806 (2012).
Shot noise thermometry of the quantum Hall edge states.
- [10] M. E. Fisher and R. E. Hartwig, Adv. Chem. Phys. **15**, 333 (1968).
Toeplitz determinants, some applications, theorems and conjectures.
- [11] E. Basor and H. Widom, J. Funct. Analysis **50**, 378 (1983).
Toeplitz and Wiener-Hopf determinants with piecewise continuous symbols.
- [12] E. L. Basor, K. E. Morrison, Linear Algebra Appl. **202**, 129 (1994).
The Fisher-Hartwig conjecture and Toeplitz eigenvalues.
- [13] T. Ehrhardt, Operator Theory: Adv. Appl. **124**, 217 (2001).
A status report on the asymptotic behavior of Toeplitz determinants with Fisher-Hartwig singularities.
- [14] P. Calabrese and F. H. L. Essler, J. Stat. Mech., P08029 (2010).
Universal corrections to scaling for block entanglement in spin-1/2 XX chains.
- [15] D. B. Gutman, Y. Gefen, and A. D. Mirlin, J. Phys. A: Math. Theor. **44**, 165003 (2011),
Non-equilibrium 1D many-body problems and asymptotic properties of Toeplitz determinants.
- [16] P. Deift, A. Its, and I. Krasovsky, Ann. of Math. **174**, 1243 (2011).
Asymptotics of Toeplitz, Hankel, and Toeplitz + Hankel determinants with Fisher-Hartwig singularities.
- [17] I. Krasovsky, *Aspects of Toeplitz determinants*, in “Boundaries and Spectra of Random Walks” (eds. D. Lenz, F. Sobieczky, W. Woess), Progr. Probability **64**, 305 (2011).
- [18] N. Kitanine, K. K. Kozłowski, J. M. Maillet, N. A. Slavnov, and V. Terras, Comm. Math. Phys. **291**, 691 (2009).
Riemann-Hilbert approach to a generalized sine kernel and applications.
K. K. Kozłowski, arXiv:0805.3902.
Truncated Wiener-Hopf operators with Fisher-Hartwig singularities.
- [19] A. G. Abanov, D. A. Ivanov, and Y. Qian, J. Phys. A: Math. Theor. **44**, 485001 (2011).
Quantum fluctuations of one-dimensional free fermions and Fisher-Hartwig formula for Toeplitz determinants.
- [20] D. A. Ivanov, A. G. Abanov, and V. V. Cheianov, J. Phys. A: Math. Theor. **46**, 085003 (2013).
Counting free fermions on a line: a Fisher-Hartwig asymptotic expansion for the Toeplitz determinant in the double-scaling limit.
- [21] D. A. Ivanov and A. G. Abanov, J. Phys. A: Math. Theor. **46**, 375005 (2013).
Fisher-Hartwig expansion for Toeplitz determinants and the spectrum of a single-particle reduced density matrix for one-dimensional free fermions.
- [22] G. Szegő, Comm. Sém. Math. Univ. Lund **228** (1952).
On certain Hermitian forms associated with the Fourier series of a positive function.
- [23] A. Böttcher and B. Silbermann, *Analysis of Toeplitz operators* (Springer, Berlin, 1990).
- [24] A. Böttcher and H. Widom, Lin. Algebra Appl. **419**, 656 (2006).
Szegő via Jacobi.
- [25] J. Keeling, I. Klich, and L. S. Levitov, Phys. Rev. Lett. **97**, 116403 (2006).
Minimal excitation states of electrons in one-dimensional wires.
- [26] M. Knap, A. Shashi, Y. Nishida, A. Imambekov, D. Abanin, and E. Demler, Phys. Rev. X **2**, 041020 (2012).
Time dependent impurity in ultracold fermions: orthogonality catastrophe and beyond.
- [27] M. Combescot and P. Nozières, J. Phys. France **32**, 913 (1971).
Infrared catastrophe and excitons in the X-ray spectra of metals.
- [28] P. Nozières and C. T. De Dominicis, Phys. Rev. **178**, 1097 (1969).
Singularities in the X-ray absorption and emission of metals. III. One-body theory exact solution.
- [29] D. A. Abanin and L. S. Levitov, Phys. Rev. Lett. **94**, 186803 (2005).
Fermi-edge resonance and tunneling in nonequilibrium electron gas.
- [30] I. Chernii, I. P. Levkivskiy, and E. V. Sukhorukov, Phys. Rev. B **90**, 245123 (2014).
Fermi-edge singularity in chiral one-dimensional systems far from equilibrium
- [31] K. S. Tikhonov and M. V. Feigelman, Phys. Rev. Lett. **105**, 067207 (2010).
Quantum spin metal state on a decorated honeycomb lat-

tice.

K. S. Tikhonov, M. V. Feigelman, and A. Yu. Kitaev, Phys. Rev. Lett. **106**, 067203 (2011).

Power-law spin correlations in a perturbed spin model on a honeycomb lattice.

- [32] I. Klich, in *Quantum Noise in Mesoscopic Physics*, ed. Yu. Nazarov (Kluwer, Dordrecht, 2003).

Full counting statistics: an elementary derivation of Levitov's formula.

- [33] E. Anderson et al, *LAPACK Users' Guide*, 3rd ed. (Soc. Ind. and Appl. Math., Philadelphia, 1999).

- [34] M. Galassi et al, *GNU Scientific Library Reference Manual*, 3rd ed. (Network Theory Ltd., Surrey, 2009),